An insight into remote sensing solutions for monitoring the *Xylella fastidiosa* bacterium that is threatening olive trees: a literature review

Marianna Hadjichristodoulou[*a,b], Christiana Papoutsa[a,b], Loukas Kanetis[a,b], Menelaos Stavrinides[a,b],

Marinos Eliades[a], Diofantos Hadjimitsis[a,b]

[*] Corresponding Author

[a] ERATOSTHENES Centre of Excellence, Franklin Roosevelt 82, 3012, Limassol, Cyprus [b] Cyprus University of Technology, Archiepiskopou Kyprianou 30, Limassol 3036, Limassol, Cyprus

ABSTRACT

Olive (*Olea europaea L.*) is a traditional crop of great socio-economic importance for Mediterranean countries, covering approximately 8,6 million hectares and providing over 90% of the world's production of olive oil. However, emerging plant pathogens threaten olive and olive oil production in the Mediterranean. Recently, olive quick decline syndrome (OQDS), an insect-borne disease caused by the bacterial pathogen *Xylella fastidiosa* (Xf), has led to the death of millions of olive trees in Italy, endangering global olive oil production. Xf colonizes the xylem vessels of the host tree being transmitted by sap feeding insects, mainly *Philaenus spumarius* (Hemiptera: Aphrophoridae). Infected trees develop symptoms that resemble symptoms from water stress due to plant vessel blockage, resulting to leaf scorching, twig, and branch dieback, and leading to tree death within a few years. To safeguard productivity and profitability of crop production, early disease detection is imperative. Remote Sensing (RS) technology offers a promising solution to challenges posed by labor-intensive, error-prone conventional field monitoring methods of plant diseases, offering insights regarding their timely spatial and temporal spread, as well their impact at early-infection stages. RS platforms, such as airborne (e.g. UAVs) and spaceborne (satellite sensors) have been utilized to monitor Xf incidence and severity. Machine-learning techniques are applied to multispectral and hyperspectral data aiming to identify affected orchards by the implicated causal agents, while specific band combinations and indices e.g. NDVI, ARVI, OSAVI have been found promising for OQDS monitoring. Summarizing, the present review examines the use of RS in Xf monitoring over the past 20 years, evaluates the effectiveness of various RS methods, identifies their benefits and limitations, and discusses future trends to enhance detection efficiency, to support effective management decisions.

Keywords: *Xylella fastidiosa (Xf)*, olive trees, Olive Quick Decline Syndrome (OQDS), Remote Sensing (RS), Integrated Pest Management

1. INTRODUCTION

Olive (*Olea europaea* L.) is one of the world's most economically significant crops, inextricably linked to the Mediterranean basin and adapted to a semi-arid temperate climate, characterized by elevated temperatures and long summer droughts. Over 48% of the global olive crop is concentrated within the Mediterranean region, spanning over 8,5 million hectares of groves, suggesting the importance of this crop for the southern part of the European Union (EU). Furthermore, besides its economic importance, traditional, low-input olive cultivation provides a substantial environmental service, via ecosystem preservation and biodiversity, since it utilizes barren,

Tenth International Conference on Remote Sensing and Geoinformation of the Environment (RSCy2024), edited by
A. Christofe, S. Michaelides, D. Hadjimitsis, C. Danezis, K. Themistocleous, N. Kyriakides, G. Schreier,
Proc. of SPIE Vol. 13212, 1321210 · © 2024 SPIE · 0277-786X · doi: 10.1117/12.3037289

stony, and steep terrains, prevailing against soil erosion [1], while it also supports the presence of social and economic networks in less-favored, remote areas of the countryside. However, the future of Mediterranean olive production faces major challenges because this region is considered a climate change 'hotspot' [2].

Currently, manifested temperature increases, and precipitation shortages have already severely affected olive production, indicating rising threats in the coming years. In addition, several anthropogenic drivers, such as the liberalization of world-trade and shifts towards intensive production schemes, characterized by high crop density and genetic uniformity, have been linked to the emergence and/or reemergence of plant pests and diseases, mainly due to the creation of new contact pathways among hosts, vectors, and pathogens [3].

Xylella fastidiosa (Xf) is an insect-borne, xylem-inhabiting, plant pathogenic bacterium native to the Americas, with a high genetic variability, holding an extremely broad pool of potential hosts (> 595) from herbaceous to trees, including agriculturally valuable crops [4],[5],[6]. Based on serological and phylogenetic studies, the species is divided into six subspecies, namely subsp. *fastidiosa*, subsp. *multiplex*, subsp. *pauca*, subsp. *taschke*, subsp. *sandyi*, and subsp. *morus*. These subspecies differ in their host rages, their geographical origins and spatial distributions [7]. It is noteworthy that currently only the subsp. *fastidiosa*, *multiplex*, and *pauca* have been detected in Europe, and several studies evaluated their potential spread [8],[9],[10], and the distribution of the main vectors of Xf in Europe [11] [12]. Although the symptoms caused by Xf can differ depending on the host plant, in general, the Xf bacterial cells block the transportation of water and soluble minerals via the xylem vessels and the infected plants show drought-related symptoms, including necrosis on the leaf margin, along with wilting and then drying of leaves, twigs and branches. Symptoms may also progress to stunted growth, resulting occasionally in plant death [5].

The economic impact of Xf-related plant diseases is considered high, making the pathogen one of the biggest threats of agriculture worldwide, categorized as a quarantine pathogen by many countries, including the EU [13]. The pathogen is responsible for socio-economically important plant diseases, such as the Pierce's disease (PD) of grapevine, the bacterial leaf scorch of shade trees, the phony peach disease, the citrus variegated chlorosis, and the almond leaf scorch [9], thus it has become a worldwide health plant concern, since disease outbreaks associated with it have been reported also in Europe, Asia and the Middle East [11]. Genetic analyses of the collected specimens suggested a close relationship of the causal agent to Xf isolates from Costa Rica, indicating a potential introduction via the importation of ornamental plants [14]. Subsequently, different introductions were reported in France, Spain, Portugal, Switzerland, and Germany on a diverse range of agricultural and ornamental plants (> 170 plant species) [15]. It is evident that Xf has the capacity to rapidly spread long distances and across borders mainly via contaminated plant material, posing major risks to disease free countries and regions, especially in the Mediterranean where olives and grapes are mostly produced. According to predictions models aiming to determine the current and forecasted distribution of Xf in the Mediterranean region under climate change conditions, the potential distribution obtained for the current time comprises Portugal, Spain, Italy, Corsica, Albania, Montenegro, Greece and Turkey, as well as the northern Africa countries and the Middle East [8].

However, as reported by [16], significant variation exists in symptoms caused by Xf and transmissibility between host species as well as cultivars. Host tolerance and/or resistance play an important role in symptom development, with plant age having an important influence on pathogen establishment and the severity of the disease.. As a result, anticipating the course of an epidemic in a novel environment is not very precise [3],[17]. In addition, the pathogen is not present uniformly in host tissue and therefore sampling detection accuracy can be low [18]. Detection based on visual inspection is further complicated, as the onset of symptoms caused by the pathogen is very slow and symptoms are not specific to the bacterium [19].

Xf is obligately spread by xylem-feeding insects of thesuperfamily Cercopoidea, with over 100 species in Europe. Nevertheless, the most widespread vector in Europe is the meadow spittlebug *Philaenus spumarius* (Hemiptera: Aphrophoridae), being also the main vector of the OQDS outbreak in Italy, while *Homalodisca vitripennis* (Hemiptera: Cicadellidae) has established long association with the epidemics of PD in North America. Other species have also demonstrated competence as Xf vectors, associated with OQDS in Italy, however exhibiting lower affinity with the olive trees and lower abundance in the specific ecosystems. Numerous uncertainties regarding the vector, pathogen and host interactions need to be studied in order to understand the

epidemiology of the pathosystem and develop optimized detection and management strategies. For example, it is recorded in that the host preferences of different developmental stages of *P. spumarius* differ, with nymphs preferring herbaceous plants, while adults shift to woody hosts in particular olive trees or *Quercus* spp. in the begging of the summer in Italy (May to July), usually found at the level of herbaceous vegetation (15-70 cm). The majority of adult *P. spumarius* frequently move by walking or jumping rather than flying [20],[21]. In addition, the host-vector interactions affect seasonal vector dynamics, while climatic conditions are shown to affect vector behavior and subsequently the disease dynamics in the groves.

Meadow spittlebug dispersal is characterized by short-distance flights, traveling with an average single flight length of 30 m and up to 100 m in a 24-hour period [22]. *P. spumarius* can spread Xf during the summer and fall, throughout the crop by secondary transmission (olive to olive), mostly because the bacterial cells linger in their mouthparts [23] [20].

Considering the complex epidemiological interactions that characterize vector-borne diseases, under variable abiotic conditions and heterogeneous landscapes, the early disease detection and assessment by sensor techniques are expected to enable more precise and effective disease management. Ground, air or space-borne RS platforms can gather digital information about pest-infected areas due to changes in the electromagnetic radiation [24] and they have been proven useful in the efficient identification, prediction and control of biotic stressors [25]. Furthermore, machine-learning technology is also applied to multispectral and hyperspectral data aiming to identify affected orchards by the implicated causal agents, while specific band combinations and indices have been found promising for OQDS monitoring. The aim of the present review was to list and summarize all the available scientific literature regarding the use of RS in the OQDS pathosystem over the past 20 years, in order to evaluate their effectiveness and discuss future trends to enhance detection efficiency and support effective management decisions.

2. METHODOLOGY

The present literature review was conducted, aiming to answer the research question of "How remote sensing technics can be utilized for detecting and monitoring the plant pathogenic bacterium, *Xylella fastidiosa*, which severely affects olive groves". The search strategy was developed to provide a comprehensive collection of relevant research studies falling within the thematic area of the review based on the methodology presented in Figure 1. Two widely respected databases, Web of Science and Google Scholar, were selected for their wide coverage of publications across various fields to assure that all relevant papers were retrieved.

To address the research question, a preliminary analysis was conducted to define the research terms, resulting to the final query across all fields. The selected terms that were used are: "olive" which was always combined with "*Xylella fastidiosa*" in all fields and the terms "satellite", "image", "UAV" or "remote sensing". At first, the search query on the Web of Science database was: in all fields "olive" AND "*Xylella fastidiosa*" AND in all fields "satellite" OR "image" OR "UAV" OR "remote sensing". The initial search was carried out in February 2023 and repeated in 15 August 2024 to ensure the inclusion of all relevant papers from the literature.

For Google Scholar, the same terms and query were applied, although the exact search structure was slightly different due to the platform's differed search capabilities and design. The above terms were used in this query: "olive" AND "*Xylella fastidiosa*" AND "satellite" OR "image" OR "UAV" OR "remote sensing". The search on Google Scholar was carried out also in February 2023. Duplicated findings and review papers were excluded, resulting in the final selection of the papers that are directly relevant to the research question set and are studied in this review.

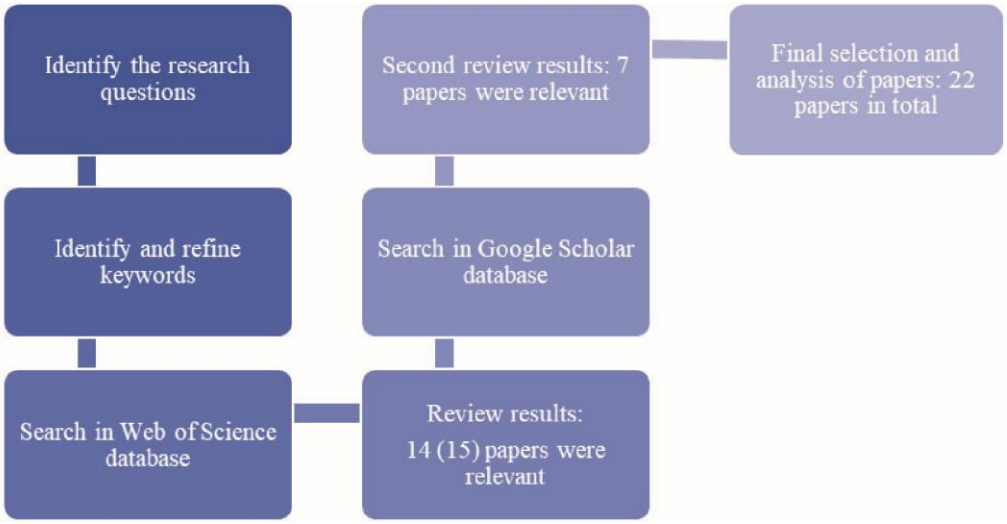

Figure 1: Review Methodology: Paper selection process

3. KEY FINDINGS

The initial search in the Web of Science database yielded 28 papers. Following the reviewing of the titles and the abstracts, 14 papers on the initial search and 1 paper from the repeated search, were found to be relevant to the research question, while 4 of them were also relevant but were excluded from our review as they were review articles. A complementary attempt was implemented using the Google Scholar database to detect any additional relevant papers. After reviewing the titles and the abstracts of the papers found using Google Scholar, 14 papers initially seemed to be relevant but at the next phase where the full papers were reviewed only seven were relevant and included in our work. Finally, using both databases we concluded with a total number of 22 papers, which were selected and analyzed, having a timeframe between 2018-2024. In the following sections (3.1 and 3.2) an analysis of the 22 papers is presented. All the papers that are analyzed in this review are listed in Table 1.

Table 1: Overview of the 22 papers that were analyzed in this review, including the authors, the titles and dates as well as their references

Author(s)	Title	Publication date	A/A and Reference No
B. Rey, N. Aleixos, S. Cubero, and J. Blasco	Xf-Rovim. A Field Robot to Detect Olive Trees Infected by *Xylella fastidiosa* Using Proximal Sensing	Jan. 2019	1. [26]
Riefolo, C., Antelmi, I., Castrignanò, A., Ruggieri, S., Galeone, C., Belmonte, A., Muolo, M.R., Ranieri, N.A., Labarile, R., Gadaleta, G., Nigro, F.	Assessment of the Hyperspectral Data Analysis as a Tool to Diagnose *Xylella fastidiosa* in the Asymptomatic Leaves of Olive Plants	Apr. 2021	2. [27]
Poblete, T., Navas-Cortes, J.A., Camino, C., Calderon, R., Hornero,	Discriminating *Xylella fastidiosa* from Verticillium dahliae infections in olive trees	Sep. 2021	3. [28]
A., Gonzalez-Dugo, V., Landa, B.B., Zarco-Tejada, P.J.	using thermal- and hyperspectral-based plant traits		

Zarco-Tejada, P.J., Camino, C., Beck, P.S.A., Calderon, R., Hornero, A., Hernández-Clemente, R., Kattenborn, T., MontesBorrego, M., Susca, L., Morelli, M., Gonzalez-Dugo, V., North, P.R.J., Landa, B.B., Boscia, D., Saponari, M., Navas-Cortes, J.A.	Previsual symptoms of *Xylella fastidiosa* infection revealed in spectral plant-trait alterations	Jun. 2018	4. [29]
Poblete, T., Camino, C., Beck, P.S.A., Hornero, A., Kattenborn, T., Saponari, M., Boscia, D., NavasCortes, J.A., Zarco-Tejada, P.J.	Detection of *Xylella fastidiosa* infection symptoms with airborne multispectral and thermal imagery: Assessing bandset reduction performance from hyperspectral analysis	Apr. 2020	5. [30]
Zarco-Tejada, P.J., Poblete, T., Camino, C., Gonzalez-Dugo, V., Calderon, R., Hornero, A., Hernandez-Clemente, R., RománÉcija, M., Velasco-Amo, M.P., Landa, B.B., Beck, P.S.A., Saponari, M., Boscia, D., NavasCortes, J.A.	Divergent abiotic spectral pathways unravel pathogen stress signals across species	Oct. 2021	6. [31]
Castrignanò, A., Belmonte, A., Antelmi, I., Quarto, R., Quarto, F., Shaddad, S., Sion, V., Muolo, M.R., Ranieri, N.A., Gadaleta, G., Bartoccetti, E., Riefolo, C., Ruggieri, S., Nigro, F.	A geostatistical fusion approach using UAV data for probabilistic estimation of *Xylella fastidiosa* subsp. pauca infection in olive trees	Jan. 2021	7. [32]
A. Belmonte, G. Gadaleta, and A. Castrignanò,	Use of Geostatistics for Multi-Scale Spatial Modeling of *Xylella fastidiosa* subsp. pauca (Xfp) Infection with Unmanned Aerial Vehicle Image	Jan. 2023	8. [33]
F. Adamo, F. Attivissimo, A. Di Nisio, M. A. Ragolia, and M. Scarpetta	A New Processing Method to Segment Olive Trees and Detect *Xylella fastidiosa* in UAVs Multispectral Images	May 2021	9. [34]
A. Di Nisio, F. Adamo, G. Acciani, and F. Attivissimo,	Fast Detection of Olive Trees Affected by *Xylella fastidiosa* from UAVs Using Multispectral Imaging	Aug. 2020	10. [35]
Castrignanò, A., Belmonte, A., Antelmi, I., Quarto, R., Quarto, F., Shaddad, S., Sion, V., Muolo, M.R., Ranieri, N.A., Gadaleta, G., Bartoccetti, E., Riefolo, C., Ruggieri, S., Nigro, F.	Semi-Automatic Method for Early Detection of *Xylella fastidiosa* in Olive Trees Using UAV Multispectral Imagery and Geostatistical-Discriminant Analysis	Dec. 2020	11. [36]
A. Corallo, F. Filieri, M. E. Latino, M. Menegoli, and M. Sarcinella	An Internet Platform to Monitor Plant Pathogens Spread: The Italian Case of Xylella	2021	12. [37]
Hornero, A., Hernández-Clemente, R., North, P.R.J., Beck, P.S.A., Boscia, D., Navas-Cortes, J.A., Zarco-Tejada, P.J.	Monitoring the incidence of *Xylella fastidiosa* infection in olive orchards using ground-based evaluations, airborne imaging spectroscopy and Sentinel-2 time series through 3-D radiative transfer modelling	Jan. 2020	13. [38]
P. Blonda, C. Tarantino, M. Scortichini, S. Maggi, M. Tarantino, and M. Adamo	Satellite monitoring of bio-fertilizer restoration in olive groves affected by *Xylella fastidiosa* subsp. pauca	Apr. 2023	14. [39]

A. Hornero, R. HernandezClemente, P. S. A. Beck, J. A. Navas-Cortes, and P. J. Zarco-Tejada	Using Sentinel-2 Imagery to Track Changes Produced by *Xylella fastidiosa* in Olive Trees	Jul. 2018	15. [40]
Semeraro, T., Buccolieri, R., Vergine, M., De Bellis, L., Luvisi, A., Emmanuel, R., Marwan, N.	Analysis of Olive Grove Destruction by *Xylella fastidiosa* Bacterium on the Land Surface Temperature in Salento Detected Using Satellite Images	Sep. 2021	16. [41]
L. Telesca, N. Abate, M. Lovallo, and R. Lasaponara	Investigating the Impact of *Xylella fastidiosa* on Olive Trees by the Analysis of MODIS Terra Satellite Evapotranspiration Time Series by Using the Fisher Information Measure and the Shannon Entropy: A Case Study in Southern Italy	Mar. 2024	17. [42]
L. Telesca, N. Abate, F. Faridani, M. Lovallo, and R. Lasaponara	Revealing traits of phytopathogenic status induced by *Xylella fastidiosa* in olive trees by analysing multifractal and informational patterns of MODIS satellite evapotranspiration data	Nov. 2023	18. [43]
L. Telesca, N. Abate, F. Faridani, M. Lovallo, and R. Lasaponara	Discerning *Xylella fastidiosa*-Infected Olive Orchards in the Time Series of MODIS Terra Satellite Evapotranspiration Data by Using the Fisher–Shannon Analysis and the Multifractal Detrended Fluctuation Analysis	Jun. 2023	19. [44]
Poblete, T., Navas-Cortes, J.A., Hornero, A., Camino, C., Calderon, R., Hernandez-Clemente, R., Landa, B.B., Zarco-Tejada, P.J.	Detection of symptoms induced by vascular plant pathogens in tree crops using highresolution satellite data: Modelling and assessment with airborne hyperspectral imagery	Sep. 2023	20. [45]
G. Santoiemma, G. Tamburini, F. Sanna, N. Mori, and L. Marini	Landscape composition predicts the distribution of Philaenus spumarius, vector of *Xylella fastidiosa*, in olive groves	Jun. 2019	21. [46]
Laneve, G., Luciani, R., Marzialetti, P., Pagnatti, S., Huang, W., Shi, Y., Dong, Y., Ye, H.	Dragon 4-satellite based analysis of diseases on permanent and row crops in Italy and China	2020	22. [47]

3.1. Ground based / *in situ* data and Airborne RS platforms

Ground based platforms and other *in situ* data are crucial for pest management by providing a non-invasive means of data collection [24]. A study developed XF-ROVIM, a robotic platform on the ground, for early detection, equipped with two digital single-lens reflex (DSLR) cameras, a multispectral camera, a thermal camera, and a hyperspectral system [26]. The XF-ROVIM efficiently collected (geolocation and synchronization) data, including 3D reconstructions and vegetation indices, inspecting the 4-ha field in max 6 hours. However, its ability to correlate structural data with the Normalized Difference Vegetation Index (NDVI), the Blue Normalized Vegetation Difference Index (BNDVI), the Leaf Area Index (LAI) and the Leaf Area Density (LAD) with disease symptoms was limited. Various models requiring spectral, spatial and structural information are needed. Moreover, another study [27] used a spectroradiometer (Field Spec IV) for the collection of hyperspectral data to detect Xf infected olives by employing statistical techniques, like Partial Least Square Regression (PLSR) and Canonical Discriminant Analysis (CDA). Selected trees were then analyzed using quantitative Polymerase Chain Reaction (qPCR) to confirm the presence of the pathogen. CDA analysis scored an accuracy of 0.67, being able to distinguish the infected trees.

Airborne RS platforms can be mounted on aircraft or other aerial vehicles to collect sample measurements in a non-destructive and non-invasive manner [48], [49]. RS techniques have been utilized in a study to

differentiate infections caused by two very destructive plant pathogens, Xf and *Verticillium dahliae* (Vd) in olive orchards [28]. The researchers utilized airborne hyperspectral and thermal high-resolution imaging, along with a three-stage Support Vector Machine (SVM) [50] model and others, to analyze datasets obtained from Italy (Xf) and Spain (Vd) and refine the detection process. Techniques such as the pure tree-crown temperature to estimate the Crop Water Stress Index (CWSI), the pure tree-crown reflectance and radiance to measure the Sun-Induced Chlorophyll Fluorescence" ($SIF_{@760}$) were used. In addition, the Photochemical Reflectance Index (PRI), the Anthocyanin Pigment Content (Anth), the Carotenoid Pigment Content (Cx+c), the LAI, the Blue-region Spectral Indices, and the NDVI were employed as well. The three-stage Machine Learning (ML) algorithm successfully distinguished infection presence from healthy trees. The Leaf Inclination Distribution Function (LIDF), the Cx+c, and the Blue index B were the spectral characteristics that separated the affected trees from those infected by Vd. Moreover, the normalized Photochemical Reflectance Index (PRI_n), the Blue/Red index (BF1), the Fluorescence Curvature Reflectance-based index (CUR), and the Carotenoid Reflectance Index (CRI_{700M}) were the parameters found to differentiate Xf from Vd. To determine whether Xf-infected olive trees could be detected through airborne imaging spectroscopy and thermography before visible symptoms become apparent, the authors of another study [29] used hyperspectral and thermal cameras on an airborne platform. The research utilized and examined various models to retrieve detailed information on leaf biochemical content, canopy structures and fluorescence efficiency. Linear ML and deep learning algorithms were employed for enhancing Receiver Operating Characteristic (ROC) analysis which is usually used to assess the classifier's efficacy [51]. Statistical analysis revealed that the most promising indices to identify infections were the Normalized Phaeophytinization Index (NPQI), CWSI, Carotenoid/Chlorophyll Ratio Index (PRI_xCI), PRI_n, SIF, BF1, the Photochemical Reflectance Index (512) (PRI_{M1}), and Photochemical Reflectance Index (670 and 570) (PRI_{M4}), CRI_{700M}, Blue index BF2, Carotenoid and Xanthophyll Pigment indices (DCabCxc), the Vogelmann Index (VOG2), and the Transformed Chlorophyll Absorption in Reflectance Index/ Optimized Soil-Adjusted Vegetation Index (TCARI/OSAVI). When they evaluated their results using the SVM model, with pigment-structure-fluorescence and temperature traits to qPCR datasets, they achieved high accuracy in distinguishing asymptomatic versus symptomatic trees and detecting the initial versus advanced disease symptoms. In addition, airborne hyperspectral and thermal imagery were used to monitor Xf in olive orchards. ML techniques, such as SVM, were also used to analyze the data derived from the aerial images [30]. The authors showed that it is important to calculate tree temperature for the detection. Still the multispectral data were important when they used a particular number of spectral bands that could differentiate the trees based on presence / absence of symptoms. The most important indices seemed to be those including the blue (calculating NPQI) and the thermal (calculating CWSI-tree temperature) bands. Some of the indices that showed best accuracy were NPQI, PRI_xCl, PRI_n, VOG2, PRI_{M4}, PRI_{M1}, TCARI/OSAVI and CRI_{7000M}, coupled with CWSI. Finally, in a subsequent study [31], airborne hyperspectral and thermal images were used to scan olive and almond trees in various regions in Italy and Spain that were affected by Xf and Vd. Abiotic stresses caused by water or nutrient deficiency results in stomatal closure and chlorosis, while the photosynthesis rate is also reduced. In practice, it is difficult to distinguish between abiotic and biotic stresses. Various physiological measurements were estimated, including leaf chlorophyll, anthocyanin, flavonoid, and nitrogen content through ground sensors and field assessments through PCR to identify the presence and type of the pathogen. Radiative Transfer (RT) model inversion was used to estimate plant traits and indices and ML algorithms like SVM to analyze the data. They determined that crops facing abiotic and biotic stresses show specific symptoms and as a result specific indices, for example, NPQI, Anth. and $SIF_{@760}$ can be used to classify Xf infection.

In a different study, UAV multispectral data, geophysical surveys using Ground Penetrating Radar (GPR) for tree trunks, visual inspection and molecular diagnostics (qPCR) were utilized, to assess the risk of Xf infection and create probability maps for better monitoring and disease prevention [32]. They suggested that it might be essential to have laboratory analysis at a small-scale to detect potential correlations within the radiometric variables indicating that the specific NIR correlations had a positive response. Furthermore, their results helped them to understand the outbreaks of bacterial / insect infections within the field (entry area), enchasing the rapid spread of the pathogen. A UAV equipped with multispectral radiometers was used in another study [33]. The authors [33] captured spectral images in several bands and applied geostatistical methods such as experimental variograms and linear model of coregionalization. Still, the Red-edge of the NIR was chosen as an indicator for the physiological state of the plant. They used the iso-frequency scale to represent spatial variability reflectance values in the Red-edge. The authors also note that it is important to use isolated images to accurately identify trees and that the use of UAV is important. In an additional study [34], a UAV with a multispectral camera was employed to identify the infected trees. For this purpose, the Linear Discriminant Analysis (LDA) was used. CIR

images derived from Blue, Green, Red, NIR and the Red-edge bands and NDVI images were further utilized. Several classifications were performed with one of them being the segmentation of the images based on the evaluation variables and those from the NIR and NDVI images. Overall, the algorithm sectioned all the trees achieving an average Dice Similarity Coefficient (DSC) of 0.66 and discrimination of infected trees was based on the LDA classification of the multispectral image pixels and not on the indices. A data fusion approach was also used in another research [35], integrating UAV multispectral data to implement detection of the infection. They generated detailed RGB, Color and Infrared (red, green, NIR) (CIR) and NDVI images using the high-resolution images taken and classified the identified trees by a segmentation algorithm, using LDA. When using NDVI, no significant differences were found between infected trees and healthy grassland but only differentiated trees from the soil. Therefore, they concluded that it is important to use a creation of a two-dimensional space. The shadows did not influence the classification algorithms. It appeared that by using five bands of multispectral images combined with LDA approach they were able to distinguish the infected trees. In a different study the authors used UAV high-resolution multispectral images obtained in a three-year period and performed geostatistical and discriminant analysis techniques [36] to provide insights to the early disease detection. In this case, Red-edge and red variables showed positive outcomes. The Red-edge gives insights on physiology, while red is correlated with the chlorophyll function of the plant. These also showed greater variability in the more stressed plants due to the presence of leaves with different degrees of dehydration, highlighting that UAV data combined with advanced data analysis can be effective. Finally, an internet platform within the Antidote Project was designed to monitor (threat, exposure and sensitivity) and forecast the risk of plant dehydration (symptom from Xf) [5]. The platform combines tools for user interaction, visualization and environmental data collection. It also provides a perspective of the olive groves by using orthophotos (precision aerial photography and satellite data). It was evident that by measuring parameters such as plant sap flow density (water and nutrient transfer), NDVI (plant health/ indicator for stress) and Vapour Pressure Deficit (VPD) (response to humidity), it was possible to monitor the disease. In addition, users could compare data from different fields and see how the crop evolves over time (e.g. seasonal trends or crop anomalies) [37]. Airborne platforms and more precisely UAVs, are preferably used more by different authors related to Xf disease affecting olive groves and its dynamics.

3.2. Spaceborne RS platforms

Large-scale monitoring in pest control is also facilitated by spaceborne platforms, usually satellites, which offer high-resolution imaging and data are processed through visualization and analysis [24]. An integrated method for large-scale detection and monitoring of Xf was developed using time-series images from the Sentinel-2A satellite over a two-year period in Apulia, Italy, [38] to observe the Disease Severity (DS) and Disease incidence (DI) of olive trees. Airborne hyperspectral images were also used for detailed analysis and model calibration purposes. The use of Vegetation Indices (VIs) from simulated spectra, six of the indices, (Atmospherically Resistant Vegetation Index (ARVI), Optimized Soil-Adjusted Veg. Index (OSAVI), Adjusted Transformed Soil-Adjusted Vegetation Index (ATSAVI), NDVI, Optimized Soil-Adjusted Veg. Index (RDVI), and Modified Simple Ratio (MSR)) were found to be efficient estimate both DS and DI, having relatively high coefficient of determination (R^2) over 0.5. In addition, OSAVI and ARVI showed better results for DI. Also, Sentinel-2 high-resolution and Pléiades very high-resolution images were utilized to investigate the impact of biofertilizer treatments on olive groves affected by Xf in another study [39]. The research compared spectral indices from treated and untreated fields. More specifically, NDVI and OSAVI indices were used to determine whether Sentinel-2 images could give reasonable and accurate results compared to the very high-resolution images, giving R^2 values ranging from 0.94 to 0.97 and 0.84 to 0.92 respectively. Examining NDVI, Normalized Difference Red-Edge (NDRE), OSAVI, and ARVI values, higher values were observed for the treated trees over a two-year period of treatment. Furthermore, treated trees had higher NDVI values than untreated ones. Further assessments were conducted [40], using multispectral Sentinel-2A and airborne hyperspectral images to monitor the spread of Xf in Apulia, Italy. The findings showed that out of all the indices tested, OSAVI, RDVI, NDVI, MSR, Normalized Difference Index (NDI), and Transformed Chlorophyll Absorption in Reflectance Index (TCARI) were positively correlated to the infection's presence, while the Optimized Soil-Adjusted Vegetation Index 1510 ($OSAVI_{1510}$) and the Modified Chlorophyll Absorption Ratio Index (MCARI) were correlated to infection severity. This demonstrates that OSAVI and $OSAVI_{1510}$ are the most relevant indices related to infection incidences and severity, respectively. Another research focused on the disease analysis on olive groves in Italy and wheat in China using high-resolution satellite imagery [47]. For the assessment of Xf in olive groves, Sentinel-2 images were used to give a better classification on how the density of the trees and their number varies

due to the presence of the infection. Veryhigh resolution images were captured by the Gaofen-1 (GF-1) satellite for validation. The olive tree density was depicted by Fraction of Vegetation Cover (FVC), as predicted by the amount of vegetation land parameters in a research area [52]. Also, the tree number was calculated by finding the average tree size according to Corine Land Cover (CLC). As the area size grows, the comparison showed that the FVC tends to overstate the number of trees in the field. This is because small vegetation will affect the FVC final score and the overall number of trees. In addition to that, by analyzing the NDVI from Sentinel-2 images with a morphological approach allowed assessing olive grove density and tree count per crop field.

Another method was used to study the effects of Xf in olive groves from 2014 to 2020 [41]. The authors utilized Landsat 8 and MODIS satellite data. They calculated Land Surface Temperature (LST) using thermal and spectral bands and used NDVI to determine the land cover emissivity. The study employed Recurrence Quantification Analysis (RQA) to examine LST's temporal evolution across different land covers. Results showed that infected olive groves had reduced effectiveness in mitigating LST. This reduction was linked to the health and vegetation structure of the olive trees and the vegetation or soil beneath. The study did not find direct effects of Xf correlated with LST, suggesting other factors, such as changes in vegetation cover, climatic conditions at the site or management practices for the infection might be influencing the LST increase. Another parameter that was observed by the research community to detect and monitor Xf in olive orchards was Evapotranspiration (ET). The water evaporation from crop soil is influenced mainly by the solar radiation that is reaching the soil. The greater the tree canopy the greater the plant transpiration [53]. In addition, another study focused on the analysis of MODIS satellite timeseries with ET to evaluate and characterize the impact of Xf in two regions in Italy [42]. They observed that the canopies of the infected trees were small, indicating lower evaporation and transpiration compared to the healthy trees. In addition, the Fisher-Shannon method was also employed to demonstrate the temporal dynamics of the data from MODIS and ROC analysis. As a result, the uninfected areas showed a greater peak in ET pixel distribution than the infected areas since the index is more sensitive when applied to the uninfected sites. The ROC analysis also showed that the Fisher parameter can provide more reliable results detecting symptoms in olive groves caused by the Xf compared to the Shannon parameter. In another study, the MODIS satellite was used to analyze ET and to estimate the association of the tree water status with Xf infection over time [43]. The Fisher-Shannon as well as the multifractional detrended fluctuation analyses were used to assess the complexity of time-series data. These methods detected decreased complexity and increased instability in ET as a marker of disease presence, indicating that there is not enough resistance to environmental disruption, due to the inner dehydration caused by the disease and therefore infected trees show similarities regardless of environmental conditions. They also found distinguishable seasonal cycles, indicating that a six-month cycle of the trees can be taken as an indication of the infection, so ET patterns may function as preliminary markers for infected trees with Xf. ET was also the main subject in another study where MODIS Terra satellite data were used to assess and separate the infected from the healthy olive trees in southern Italy [44]. There were variations in the ET time series measurements, suggesting that the areas showing less diversity and compositionality appear to be infected because they fail to meet the nutrient requirements of the plant due to the infection. Still, ROC analysis gave positive results, showing that the multifractal structures could be more ideal for ET. Thus, ET could be an efficient tool for the identification and monitoring of Xf.

Furthermore, in a different study, the airborne hyperspectral, Worldview-2 and Worldview-3 multispectral, and thermal images were used [45] to identify early-stage of the infections by Xf and Vd in both olive and almond trees and various indices were calculated to detect the symptoms. Sentinel-2 data were also used for calibration purposes. ML algorithms, such as SVM and RF, were used to classify symptom severity. When the thermal indicator CWSI was used, it upgraded the disease detection precision rates by 10-15%. In addition, NPQI showed great importance but decreased as the severity of the symptoms increased. Also, the factor that caused errors in the diagnosis was the number of trees in the early stage of the disease's development. The overall accuracy in the disease detection was between 0.63-0.83 (R^2). Lastly, the influence of landscape composition on *P. spumarius* (vector of Xf) distribution within olive groves was employed [46] utilizing high-resolution satellite images (Google earth Engine Pro) for vector monitoring The findings show that, the composition of the landscape around the olive orchards and the agricultural management may have an impact on the likelihood of the spread of the infection, highlighting the significance of managing landscape elements to control disease spread via the vector.From the analysis that was conducted, it was depicted that Sentinel-2 and MODIS satellites are the most commonly used RS spaceborne platforms for enhancing the research of Xf infections and can provide vital data. Table 2 provides a concise overview of the types of the sensors, data and

primary indices / parameters utilized in the studies, along with their corresponding references. The selected papers used in the current review are fully listed in Table 1.

Table 2: A summary of RS platforms that are used in the 22 selected papers for monitoring and detection of Xf infections in olive groves.

Ground based platforms / In situ data			
Sensor type	Data type	Main indices/ parameters	Reference
Ground-based robot	Thermal, Hyperspectral Multispectral DSLR cameras, GPS	BNDVI, NDVI, LAI, LAD	[26]
Field Spec IV spectroradiometer	Hyperspectral	PRI, VOG2, Stress VIs	[27]
GPR for trunks	Multispectral	Green, Red-Edge and Red, NIR - Red-Edge bands	[32]
Airborne platforms			
Sensor type	Data type	Main indices/ parameters	Reference
Airborne	Hyperspectral, Thermal	LIDF, Cx+c, blue index B, CWSI, PRI_n, SIF, BF1	[28]
Airborne	Hyperspectral, Thermal	NPQI, CWSI, PRIxCI, PRI_n, SIF, BF1, PRI_{M1}, CRI_{700M}, Blue index BF2, PRI_{M4}, DCabCxc, TCARI/OSAVI	[29]
Airborne	Hyperspectral, Thermal	NPQI, PRIxCl, PRI_n, VOG2, PRI_{M4}, PRI_{M1}, TCARI/OSAVI, CRI_{7000M}, CWSI	[30]
Airborne	Hyperspectral, Multispectral, Thermal	Chlorophyll content (Ca+b), carotenoid content (Cx+c), Anth., mesophyll structure (N), LAI, LIDF, CWSI, SIF@760, NPQI	[31]
UAV	Multispectral	Green, Red-Edge and Red, NIR - Red-Edge bands	[32]
UAV	Multispectral	NIR band	[33]
UAV	Multispectral	NDVI, NIR, blue, green, red, ref-edge	[34]
UAV	Multispectral	NDVI, CIR, RGB	[35]
UAV	Multispectral	-	[36]
Precision aerial photography	-	NDVI, VPD, Plant sap flow density	[37]
Airborne	Hyperspectral	ARVI, OSAVI, ATSAVI, NDVI, RDVI, MSR	[38]
Airborne	Hyperspectral	OSAVI, RDVI, NDVI, MSR, NDI, TCARI, $OSAVI_{1510}$, MCARI	[40]
Airborne	Hyperspectral, Thermal	NPQI, CWSI, PRI_n, CUR, LAI, Anth, $SIF_{@760}$, $LIDF_a$, C_{a+b} , CRI_{700M}	[45]
Spaceborne platforms			
Sensor type	Data type	Main indices/ parameters	Reference
Satellite data	-	NDVI, VPD, Plant sap flow density	[37]

Sentinel-2	Multispectral	ARVI, OSAVI, ATSAVI, NDVI, RDVI, MSR	[38]
Sentinel-2 and Pleiades	Multispectral	NDVI, OSAVI, NDRE, ARVI	[39]
Sentinel-2	Multispectral	OSAVI, RDVI, NDVI, MSR, NDI, TCARI, $OSAVI_{1510}$, MCARI	[40]
Landsat 8 and MODIS	Multispectral, Thermal	LST, NDVI	[41]
MODIS	Multispectral	ET	[42]
MODIS	Multispectral	ET	[43]
MODIS	Multispectral	ET	[44]
Worldview-2 and Worldview-3 and Sentinel-2 (validation)	Multispectral	NPQI, CWSI, PRI_n, CUR, LAI, Anth, $SIF_{@760}$, $LIDF_a$, C_{a+b} , CRI_{700M}	[45]
Multiple satellite platforms	Google Earth Engine	-	[46]
Sentinel-2 and GF-1 (validation)	Multispectral	NDVI, Carotenoid indices	[47]

4. CONCLUSION

Spaceborne and airborne platforms are widely utilized in literature for detecting Xf infections in olive groves. Sentinel-2 and MODIS satellites are the most used spaceborne platforms, while airborne prevailed the category of airborne platforms. Vegetation indices like PRI, NDVI, OSAVI and more, are shown to be frequently employed in these studies. Notably, CWSI, SIF, and ET-related indicators provide crucial information about plant moisture levels, highlighting the internal dehydration caused by the disease. This information is valuable for assessing the infection state and exploring improvement/ management strategies. In addition to that, the combination of indices and other algorithms and models like SVM, LDA etc. enhances the accuracy of results and offers deeper insights into the progression of the disease and its severity. It is essential to recognize that each study area has unique characteristics and conditions, which can affect experimental outcomes despite being infected by the same disease. Future research should focus on the variability of LST under changing climatic conditions and to enhance its relationship with the disease. Furthermore, some studies suggest that hyperspectral images and other sensor types could be pivotal for disease detection in olive orchards, an aspect that can be further investigated. Finally, there is a noticeable lack of quantitative estimation of critical epidemiological variables, such as transmission rates, asymptomatic phase duration, and the timeline until the plant becomes completely dry and dies, that can relate with remote sensing data, and which are essential for risk assessment and pest management.

ACKNOWLEDGMENTS

The authors acknowledge the ‘EXCELSIOR’: ERATOSTHENES: Excellence Research Centre for Earth Surveillance and Space-Based Monitoring of the Environment H2020 Widespread Teaming project (www.excelsior2020.eu). The ‘EXCELSIOR’ project has received funding from the European Union’s Horizon 2020 research and innovation programme under Grant Agreement No 857510, from the Government of the Republic of Cyprus through the Directorate General for the European Programmes, Coordination and Development and the Cyprus University of Technology.

The present work was carried out in the framework of CERBERUS project that has received funding from the Horizon Europe HORIZON-CL6-2023-GOVERNANCE-01-16- HORIZON Research and Innovation Actions, under Grant Agreement No 101134878.

REFERENCES

[1] E. Lantero *et al.*, "Effect of local and landscape factors on abundance of ground beetles and assessment of their role as biocontrol agents in the olive growing area of southeastern Madrid, Spain," *BioControl*, vol. 64, no. 6, pp. 685–696, Dec. 2019, doi: 10.1007/s10526-019-09974-w.

[2] D. Kaniewski *et al.*, "Climate change threatens olive oil production in the Levant," *Nat. Plants*, vol. 9, no. 2, pp. 219–227, Jan. 2023, doi: 10.1038/s41477-022-01339-z.

[3] F. Occhibove *et al.*, "Eco-Epidemiological Uncertainties of Emerging Plant Diseases: The Challenge of Predicting *Xylella fastidiosa* Dynamics in Novel Environments," *Phytopathology®*, vol. 110, no. 11, pp. 1740–1750, Nov. 2020, doi: 10.1094/PHYTO-03-20-0098-RVW.

[4] N. Potnis *et al.*, "Patterns of inter- and intrasubspecific homologous recombination inform ecoevolutionary dynamics of *Xylella fastidiosa*," *ISME J.*, vol. 13, no. 9, pp. 2319–2333, Sep. 2019, doi: 10.1038/s41396-019-0423-y.

[5] V. Trkulja, A. Tomić, R. Iličić, M. Nožinić, and T. P. Milovanović, "*Xylella fastidiosa* in Europe: From the Introduction to the Current Status," *Plant Pathol. J.*, vol. 38, no. 6, pp. 551–571, Dec. 2022, doi: 10.5423/PPJ.RW.09.2022.0127.

[6] K. Schneider *et al.*, "Impact of *Xylella fastidiosa* subspecies *pauca* in European olives," *Proc. Natl. Acad. Sci.*, vol. 117, no. 17, pp. 9250–9259, Apr. 2020, doi: 10.1073/pnas.1912206117.

[7] L. Nunney *et al.*, "Recent Evolutionary Radiation and Host Plant Specialization in the *Xylella fastidiosa* Subspecies Native to the United States," *Appl. Environ. Microbiol.*, vol. 79, no. 7, pp. 2189–2200, Apr. 2013, doi: 10.1128/AEM.03208-12.

[8] L. Bosso, M. Di Febbraro, G. Cristinzio, A. Zoina, and D. Russo, "Shedding light on the effects of climate change on the potential distribution of *Xylella fastidiosa* in the Mediterranean basin," *Biol. Invasions*, vol. 18, no. 6, pp. 1759–1768, Jun. 2016, doi: 10.1007/s10530-016-1118-1.

[9] EFSA Panel on Plant Health (PLH) *et al.*, "Update of the Scientific Opinion on the risks to plant health posed by *Xylella fastidiosa* in the EU territory," *EFSA J.*, vol. 17, no. 5, May 2019, doi: 10.2903/j.efsa.2019.5665.

[10] M. Godefroid, A. Cruaud, J.-C. Streito, J.-Y. Rasplus, and J.-P. Rossi, "*Xylella fastidiosa*: climate suitability of European continent," *Sci. Rep.*, vol. 9, no. 1, p. 8844, Jun. 2019, doi: 10.1038/s41598-01945365-y.

[11] M. Godefroid *et al.*, "Climate tolerances of Philaenus spumarius should be considered in risk assessment of disease outbreaks related to *Xylella fastidiosa*," *J. Pest Sci.*, vol. 95, no. 2, pp. 855–868, Mar. 2022, doi: 10.1007/s10340-021-01413-z.

[12] M. Godefroid and J. M. Durán, "Composition of landscape impacts the distribution of the main vectors of *Xylella fastidiosa* in southern Spain," *J. Appl. Entomol.*, vol. 146, no. 6, pp. 666–675, Jul. 2022, doi: 10.1111/jen.13003.

[13] K. Schneider *et al.*, "Impact of *Xylella fastidiosa* subspecies *pauca* in European olives," *Proc. Natl. Acad. Sci.*, vol. 117, no. 17, pp. 9250–9259, Apr. 2020, doi: 10.1073/pnas.1912206117.

[14] European Food Safety Authority (EFSA), A. Delbianco, D. Gibin, L. Pasinato, D. Boscia, and M. Morelli, "Update of the Xylella spp. host plant database – systematic literature search up to 30 June 2022," *EFSA J.*, vol. 21, no. 1, Jan. 2023, doi: 10.2903/j.efsa.2023.7726.

[15] European Food Safety Authority (EFSA), A. Loomans, M. Diakaki, M. Kinkar, M. Schenk, and S. Vos, "Pest survey card on Bactrocera dorsalis," *EFSA Support. Publ.*, vol. 16, no. 9, Sep. 2019, doi: 10.2903/sp.efsa.2019.EN-1714.

[16] E. Sabella *et al.*, "Xylem cavitation susceptibility and refilling mechanisms in olive trees infected by *Xylella fastidiosa*," *Sci. Rep.*, vol. 9, no. 1, p. 9602, Jul. 2019, doi: 10.1038/s41598-019-46092-0.

[17] C. Roper, C. Castro, and B. Ingel, "*Xylella fastidiosa*: bacterial parasitism with hallmarks of commensalism," *Curr. Opin. Plant Biol.*, vol. 50, pp. 140–147, Aug. 2019, doi: 10.1016/j.pbi.2019.05.005.

[18] A. H. Purcell and S. R. Saunders, "Fate of Pierce's Disease Strains of *Xylella fastidiosa* in Common Riparian Plants in California," *Plant Dis.*, vol. 83, no. 9, pp. 825–830, Sep. 1999, doi: 10.1094/PDIS.1999.83.9.825.

[19] J. Rapicavoli, B. Ingel, B. Blanco-Ulate, D. Cantu, and C. Roper, "*Xylella fastidiosa* : an examination of a re-emerging plant pathogen," *Mol. Plant Pathol.*, vol. 19, no. 4, pp. 786–800, Apr. 2018, doi: 10.1111/mpp.12585.

[20] N. Bodino *et al.*, “Spittlebugs of Mediterranean Olive Groves: Host-Plant Exploitation throughout the Year,” *Insects*, vol. 11, no. 2, p. 130, Feb. 2020, doi: 10.3390/insects11020130.
[21] N. Bodino *et al.*, “Phenology, seasonal abundance and stage-structure of spittlebug (Hemiptera: Aphrophoridae) populations in olive groves in Italy,” *Sci. Rep.*, vol. 9, no. 1, p. 17725, Nov. 2019, doi: 10.1038/s41598-019-54279-8.
[22] D. Cornara *et al.*, “An overview on the worldwide vectors of *Xylella fastidiosa*,” *Entomol. Gen.*, vol. 39, no. 3–4, pp. 157–181, Dec. 2019, doi: 10.1127/entomologia/2019/0811.
[23] N. Bodino *et al.*, “Dispersal of *Philaenus spumarius* (Hemiptera: Aphrophoridae), a Vector of *Xylella fastidiosa* , in Olive Grove and Meadow Agroecosystems,” *Environ. Entomol.*, vol. 50, no. 2, pp. 267–279, Apr. 2021, doi: 10.1093/ee/nvaa140.
[24] C. Keswani, Ed., *Bioeconomy for Sustainable Development*. Singapore: Springer Singapore, 2020. doi: 10.1007/978-981-13-9431-7.
[25] N. M. Abd El-Ghany, S. E. Abd El-Aziz, and S. S. Marei, “A review: application of remote sensing as a promising strategy for insect pests and diseases management,” *Environ. Sci. Pollut. Res.*, vol. 27, no. 27, pp. 33503–33515, Sep. 2020, doi: 10.1007/s11356-020-09517-2.
[26] B. Rey, N. Aleixos, S. Cubero, and J. Blasco, “Xf-Rovim. A Field Robot to Detect Olive Trees Infected by *Xylella fastidiosa* Using Proximal Sensing,” *Remote Sens.*, vol. 11, no. 3, p. 221, Jan. 2019, doi: 10.3390/rs11030221.
[27] C. Riefolo *et al.*, “Assessment of the Hyperspectral Data Analysis as a Tool to Diagnose *Xylella fastidiosa* in the Asymptomatic Leaves of Olive Plants,” *Plants*, vol. 10, no. 4, p. 683, Apr. 2021, doi: 10.3390/plants10040683.
[28] T. Poblete *et al.*, “Discriminating *Xylella fastidiosa* from Verticillium dahliae infections in olive trees using thermal- and hyperspectral-based plant traits,” *ISPRS J. Photogramm. Remote Sens.*, vol. 179, pp. 133–144, Sep. 2021, doi: 10.1016/j.isprsjprs.2021.07.014.
[29] P. J. Zarco-Tejada *et al.*, “Previsual symptoms of *Xylella fastidiosa* infection revealed in spectral planttrait alterations,” *Nat. Plants*, vol. 4, no. 7, pp. 432–439, Jun. 2018, doi: 10.1038/s41477-018-0189-7.
[30] T. Poblete *et al.*, “Detection of *Xylella fastidiosa* infection symptoms with airborne multispectral and thermal imagery: Assessing bandset reduction performance from hyperspectral analysis,” *ISPRS J. Photogramm. Remote Sens.*, vol. 162, pp. 27–40, Apr. 2020, doi: 10.1016/j.isprsjprs.2020.02.010.
[31] P. J. Zarco-Tejada *et al.*, “Divergent abiotic spectral pathways unravel pathogen stress signals across species,” *Nat. Commun.*, vol. 12, no. 1, p. 6088, Oct. 2021, doi: 10.1038/s41467-021-26335-3.
[32] A. Castrignanò *et al.*, “A geostatistical fusion approach using UAV data for probabilistic estimation of *Xylella fastidiosa* subsp. pauca infection in olive trees,” *Sci. Total Environ.*, vol. 752, p. 141814, Jan. 2021, doi: 10.1016/j.scitotenv.2020.141814.
[33] A. Belmonte, G. Gadaleta, and A. Castrignanò, “Use of Geostatistics for Multi-Scale Spatial Modeling of *Xylella fastidiosa* subsp. pauca (Xfp) Infection with Unmanned Aerial Vehicle Image,” *Remote Sens.*, vol. 15, no. 3, p. 656, Jan. 2023, doi: 10.3390/rs15030656.
[34] F. Adamo, F. Attivissimo, A. Di Nisio, M. A. Ragolia, and M. Scarpetta, “A New Processing Method to Segment Olive Trees and Detect *Xylella fastidiosa* in UAVs Multispectral Images,” in *2021 IEEE International Instrumentation and Measurement Technology Conference (I2MTC)*, Glasgow, United Kingdom: IEEE, May 2021, pp. 1–6. doi: 10.1109/I2MTC50364.2021.9459835.
[35] A. Di Nisio, F. Adamo, G. Acciani, and F. Attivissimo, “Fast Detection of Olive Trees Affected by *Xylella fastidiosa* from UAVs Using Multispectral Imaging,” *Sensors*, vol. 20, no. 17, p. 4915, Aug. 2020, doi: 10.3390/s20174915.
[36] A. Castrignanò *et al.*, “Semi-Automatic Method for Early Detection of *Xylella fastidiosa* in Olive Trees Using UAV Multispectral Imagery and Geostatistical-Discriminant Analysis,” *Remote Sens.*, vol. 13, no. 1, p. 14, Dec. 2020, doi: 10.3390/rs13010014.
[37] Department of Innovation Engineering, University of Salento, Lecce 73100, Italy, A. Corallo, F. Filieri, M. E. Latino, M. Menegoli, and M. Sarcinella, “An Internet Platform to Monitor Plant Pathogens Spread: The Italian Case of Xylella,” *J. Commun.*, pp. 204–209, 2021, doi: 10.12720/jcm.16.6.204-209.
[38] A. Hornero *et al.*, “Monitoring the incidence of *Xylella fastidiosa* infection in olive orchards using ground-based evaluations, airborne imaging spectroscopy and Sentinel-2 time series through 3-D radiative transfer modelling,” *Remote Sens. Environ.*, vol. 236, p. 111480, Jan. 2020, doi: 10.1016/j.rse.2019.111480.
[39] P. Blonda, C. Tarantino, M. Scortichini, S. Maggi, M. Tarantino, and M. Adamo, “Satellite monitoring of bio-fertilizer restoration in olive groves affected by *Xylella fastidiosa* subsp. pauca,” *Sci. Rep.*, vol. 13, no. 1, p. 5695, Apr. 2023, doi: 10.1038/s41598-023-32170-x.

[40] A. Hornero, R. Hernandez-Clemente, P. S. A. Beck, J. A. Navas-Cortes, and P. J. Zarco-Tejada, "Using Sentinel-2 Imagery to Track Changes Produced by *Xylella fastidiosa* in Olive Trees," in *IGARSS 2018 - 2018 IEEE International Geoscience and Remote Sensing Symposium*, Valencia: IEEE, Jul. 2018, pp. 9060–9062. doi: 10.1109/IGARSS.2018.8517697.

[41] T. Semeraro *et al.*, "Analysis of Olive Grove Destruction by *Xylella fastidiosa* Bacterium on the Land Surface Temperature in Salento Detected Using Satellite Images," *Forests*, vol. 12, no. 9, p. 1266, Sep. 2021, doi: 10.3390/f12091266.

[42] L. Telesca, N. Abate, M. Lovallo, and R. Lasaponara, "Investigating the Impact of *Xylella fastidiosa* on Olive Trees by the Analysis of MODIS Terra Satellite Evapotranspiration Time Series by Using the Fisher Information Measure and the Shannon Entropy: A Case Study in Southern Italy," *Remote Sens.*, vol. 16, no. 7, p. 1242, Mar. 2024, doi: 10.3390/rs16071242.

[43] L. Telesca, N. Abate, F. Faridani, M. Lovallo, and R. Lasaponara, "Revealing traits of phytopathogenic status induced by *Xylella fastidiosa* in olive trees by analysing multifractal and informational patterns of MODIS satellite evapotranspiration data," *Phys. Stat. Mech. Its Appl.*, vol. 629, p. 129163, Nov. 2023, doi: 10.1016/j.physa.2023.129163.

[44] L. Telesca, N. Abate, F. Faridani, M. Lovallo, and R. Lasaponara, "Discerning *Xylella fastidiosa*-Infected Olive Orchards in the Time Series of MODIS Terra Satellite Evapotranspiration Data by Using the Fisher–Shannon Analysis and the Multifractal Detrended Fluctuation Analysis," *Fractal Fract.*, vol. 7, no. 6, p. 466, Jun. 2023, doi: 10.3390/fractalfract7060466.

[45] T. Poblete *et al.*, "Detection of symptoms induced by vascular plant pathogens in tree crops using highresolution satellite data: Modelling and assessment with airborne hyperspectral imagery," *Remote Sens. Environ.*, vol. 295, p. 113698, Sep. 2023, doi: 10.1016/j.rse.2023.113698.

[46] G. Santoiemma, G. Tamburini, F. Sanna, N. Mori, and L. Marini, "Landscape composition predicts the distribution of Philaenus spumarius, vector of *Xylella fastidiosa*, in olive groves," *J. Pest Sci.*, vol. 92, no. 3, pp. 1101–1109, Jun. 2019, doi: 10.1007/s10340-019-01095-8.

[47] G. Laneve *et al.*, "Dragon 4-satellite based analysis of diseases on permanent and row crops in Italy and China," *Journal of Geodesy and Geoinformation Science*, vol. 3(4), pp. 107–118, 2020, doi: 10.11947/j.JGGS.2020.0411.

[48] Y. Lan, Y. Huang, D. E. Martin, and W. C. Hoffmann, "Development of an Airborne Remote Sensing System for Crop Pest Management: System Integration and Verification," *Appl. Eng. Agric.*, vol. 25, no. 4, pp. 607–615, 2009, doi: 10.13031/2013.27458.

[49] T. Boonupara, P. Udomkun, E. Khan, and P. Kajitvichyanukul, "Airborne Pesticides from Agricultural Practices: A Critical Review of Pathways, Influencing Factors, and Human Health Implications," *Toxics*, vol. 11, no. 10, p. 858, Oct. 2023, doi: 10.3390/toxics11100858.

[50] M. A. Hearst, S. T. Dumais, E. Osuna, J. Platt, and B. Scholkopf, "Support vector machines," *IEEE Intell. Syst. Their Appl.*, vol. 13, no. 4, pp. 18–28, Jul. 1998, doi: 10.1109/5254.708428.

[51] T. Fawcett, "An introduction to ROC analysis," *Pattern Recognit. Lett.*, vol. 27, no. 8, pp. 861–874, Jun. 2006, doi: 10.1016/j.patrec.2005.10.010.

[52] S. Zhang, H. Chen, Y. Fu, H. Niu, Y. Yang, and B. Zhang, "Fractional Vegetation Cover Estimation of Different Vegetation Types in the Qaidam Basin," *Sustainability*, vol. 11, no. 3, p. 864, Feb. 2019, doi: 10.3390/su11030864.

[53] R. G. Allen, *Crop evapotranspiration: guidelines for computing crop water requirements*. in FAO irrigation and drainage paper, no. 56. Rome: Food and Agriculture Organization of the United Nations, 1998.